



Consumption of atmospheric O₂ in an Urban Area of Tokyo, Japan derived from continuous observations of O₂ and CO₂ concentrations and CO₂ flux

Shigeyuki Ishidoya¹, Hirofumi Sugawara², Yukio Terao³, Naoki Kaneyasu¹,
5 Nobuyuki Aoki¹, Kazuhiro Tsuboi⁴, and Hiroaki Kondo¹

¹National Institute of Advanced Industrial Science and Technology (AIST), Tsukuba 305-8569, Japan

²Department of Earth and Ocean Sciences, National Defense Academy of Japan, Yokosuka 239-8686, Japan

³National Institute for Environmental Studies, Tsukuba 305-8506, Japan

⁴Meteorological Research Institute, Tsukuba 305-0052, Japan

10 *Correspondence to:* Shigeyuki Ishidoya (s-ishidoya@aist.go.jp)

Abstract. In order to estimate the atmospheric O₂ consumption in a megacity, continuous observations of atmospheric O₂ and CO₂ concentrations and of CO₂ flux have been carried out simultaneously at the Yoyogi (YYG) site in middle of Tokyo, Japan since March 2016. An average O₂:CO₂ exchange ratio for net turbulent O₂ and CO₂ fluxes (OR_F) between the urban area and the overlying atmosphere was obtained based on an aerodynamic method using the observed O₂ and CO₂ concentrations. The yearly mean OR_F was found to be 1.62, falling within the range of the average OR values of liquid and gas fuels. Seasonally different diurnal OR_F cycles at YYG indicated that the consumption of gas fuels was larger in the winter than that in the summer, especially in the morning and late in the evening. By using the OR_F and CO₂ flux values, the annual mean O₂ consumption rate was estimated to be -16.3 μmol m⁻²s⁻¹, which is more than 350 times larger than the global mean atmospheric O₂ consumption rate (about -4 μmol yr⁻¹), implying that our life in a megacity is far from sustainable from a viewpoint of the conservation of atmospheric O₂.

1. Introduction

Precise observation of the atmospheric O₂ concentration (O₂/N₂ ratio) has been carried out since the early 1990s to elucidate the global CO₂ cycle (Keeling and Shertz, 1992). The approach is based on the -O₂:CO₂ exchange ratios (Oxidative Ratio; OR = -ΔO₂ΔCO₂⁻¹ mol mol⁻¹) for the terrestrial biospheric activities and fossil fuel combustion. The OR value of 1.1 has been used widely for the terrestrial biospheric O₂ and CO₂ fluxes (Severinghaus, 1995). On the other hand, the OR of 1.95 for gaseous fuels, 1.44 for oil and other liquid fuels, and 1.17 for coal or solid fuels are usually used (Keeling, 1988). Therefore, OR is a useful indicator for cause(s) of the observed variations in the atmospheric O₂ and CO₂ concentrations. The atmospheric CO₂ concentration has been observed not only at remote sites such as Mauna Loa (19.5 °N, 155.6 °W), Hawaii, U.S.A. to capture a baseline variation in the background air (e.g. Keeling et al., 2011) but also recently in urban areas to estimate CO₂ emissions locally from fossil fuel combustion (e.g. Mitchell et al., 2018). For the latter purpose,



simultaneous observations of the atmospheric O₂ and CO₂ concentrations should provide important insight in separating out the respective contributions of the gaseous, liquid and solid fuels to the urban CO₂ emission.

Steinbach et al. (2011) estimated a global dataset of spatial and temporal variations of OR for the fossil fuel combustion using the EDGAR (Emission Database for Global Atmospheric Research) inventory and fossil fuel consumption data from the UN energy statistics. The statistically estimated OR should be validated by observed OR, however observations of the atmospheric O₂ concentration in urban areas are still limited (e.g. van der Laan et al., 2014; Goto et al., 2013). Moreover, simultaneous observations of the OR and CO₂ flux between an urban area and the overlying atmosphere have never been reported before. Observations of the CO₂ flux have been carried out at various urban stations such as, London, UK (Ward et al., 2013), Mexico City, Mexico (Velasco et al., 2009), Beijing, China (Song and Wang, 2012), and Tokyo, Japan (Hirano et al., 2015), allowing us to observe urban CO₂ emission directly in the flux footprint. Therefore, if the OR for the net turbulent O₂ and CO₂ fluxes (hereafter referred to as “OR_F”) is observed, then the information can be used to separate out the contributions of the gaseous, liquid, and solid fuels, and the terrestrial biospheric activities to the observed CO₂ flux. From the measurements, it also becomes possible to observe the urban O₂ flux by multiplying the CO₂ flux by OR_F.

In this paper, we present firstly the simultaneous observational results of the O₂ and CO₂ concentrations and the CO₂ flux in the urban area of Tokyo, Japan. From a relationship between the vertical gradients of the observed O₂ and CO₂ concentrations, we derive OR_F based on an aerodynamic method (Yamamoto et al., 1999). The present paper follows Ishidoya et al. (2015) who reported OR_F for the O₂ and CO₂ fluxes between a forest canopy and the overlying atmosphere. We also compare the observed OR_F with the OR value of the overlying atmosphere above the urban canopy (hereafter referred to as “OR_{atm}”) to highlight the characteristics of the O₂ and CO₂ exchange processes in the urban canopy air at the YYG site. Finally, we discuss the cause(s) of the urban O₂ flux in a megacity like Tokyo.

2. Experimental procedures

2.1 Site description

In order to observe the atmospheric O₂ and CO₂ concentrations and CO₂ flux between the urban area and the overlying atmosphere, the instruments were installed on a roof-top tower of Tokai University (52 m above ground, 25 m above roof) at Yoyogi (YYG; 35.66°N, 139.68°E), Tokyo, Japan. The YYG site is a mid-rise residential area and located in the northern part of Shibuya ward, Tokyo. Figure 1 shows the location of the YYG site and the flux footprints averaged for summer and winter runs, calculated by the model of Kljun et al. (2004). The main land-cover around the site is characterized by low- to mid-rise residential buildings with a mean height of 9 m. The population density in this area is 16,600 persons km⁻². At the YYG site, prevailing wind is from SW in the summer and NW in the winter. The flux footprint includes vegetated area of 9% in the summer and 2% in the winter.



2.2 Continuous measurements of the atmospheric O₂ and CO₂ concentrations and CO₂ flux

Observations of the atmospheric O₂ and CO₂ concentrations have been carried out at the YYG site using a continuous measurement system employing a paramagnetic O₂ analyzer (POM-6E, Japan Air Liquid) and a non-dispersive infrared CO₂ analyzer (NDIR; Li-820, LI-COR) since March 2016. The O₂ concentration is reported as the O₂/N₂ ratio in per meg:

$$\delta(O_2/N_2) = \left[\frac{(O_2/N_2)_{\text{sample}}}{(O_2/N_2)_{\text{standard}}} - 1 \right] \times 10^6 \quad (\text{eq.1})$$

where the subscripts ‘sample’ and ‘standard’ indicate the sample air and the standard gas, respectively. Because O₂ is about 20.94 % of air by volume (Tohjima et al., 2005a), the addition of 1 μmol of O₂ to 1 mol of dry air increases δ(O₂/N₂) by 4.8 per meg (=1/0.2094). If CO₂ were to be converted one-for-one into O₂, this would cause an increase of 4.8 per meg of δ(O₂/N₂), equivalent to an increase of 1 μmol mol⁻¹ of O₂ for each 1 μmol mol⁻¹ decrease in CO₂. Therefore, the ratio of 4.8 per meg/μmol mol⁻¹ was used to convert the observed δ(O₂/N₂) to O₂ concentration relative to an arbitrary reference point. In this study, δ(O₂/N₂) of each air sample was determined against our primary standard air (Cylinder No. CRC00045; AIST-scale) using a mass spectrometer (Thermo Scientific Delta-V) (Ishidoya and Murayama, 2014).

In this study, sample air was taken at the tower heights of 52 m and 37 m using a diaphragm pump at a flow rate higher than 10 L min⁻¹. The sample air taken from 52 m and 37 m were introduced into the analyzers through a water trap cooled to -80°C at a flow rate of 100 mL min⁻¹ by stabilizing the pressure to an order of 10⁻¹ Pa, and measured for 10 minutes at each height. After 9 measurement cycles (90 minutes), high-span standard gas, prepared by adding appropriate amounts of pure O₂ or N₂ to industrially prepared CO₂ standard air, was introduced into the analyzers with the same flow rate and pressure as the sample air and measured for 5 minutes, and then low-span standard gas was measured by the same procedure. The dilution effects on the O₂ mole fraction measured by the paramagnetic analyzer due to changes in CO₂ and Ar of the sample air or standard gas were corrected experimentally. The analytical reproducibility of the O₂/N₂ ratio (CO₂ concentration) achieved by the system was about 5 and 3 per meg (0.06 and 0.04 μmol mol⁻¹) for 2 and 30 minute average values, respectively. The reproducibility of the O₂/N₂ ratio was equivalent to those of O₂ concentrations of 1.0 μmol mol⁻¹ for 2 minute average and 0.6 μmol mol⁻¹ for 30 minute average. Details of the continuous measurement system used are given in Ishidoya et al. (2017).

It should be noted that the gravimetrically prepared air-based CO₂ standard gas system with uncertainties of ±0.13 μmol mol⁻¹ on TU-10 scale (Nakazawa et al., 1991) was used to determine CO₂ concentration in this study. The highest concentration of the gravimetrically standard gas was about 450 μmol mol⁻¹, while CO₂ concentrations of more than 600 μmol mol⁻¹ were observed in this study. Therefore, we compared the NDIR-based CO₂ concentrations observed in this study with those observed by using Cavity Ring-Down Spectroscopy (CRDS; G2401, Picarro) on NIES-09 scale (Machida et al., 2011) at the YYG site (our unpublished data). Although the highest CO₂ concentration of the gravimetrically standard for the NIES-09 scale is similar to that of the TU-10 scale, the span-difference of CO₂ concentration between the TU-10 and NIES-09 scales



was confirmed to be within 1% for a range of 410-560 $\mu\text{mol mol}^{-1}$, as determined by applying a geometric mean regression with a correlation coefficient of 0.978 (Miller and Tans, 2003). On the other hand, the span-difference of O_2 concentration between the AIST-scale and the highly precise O_2 standard gases developed by Aoki et al. (2019) was confirmed to be within 95 0.2%. Therefore, the uncertainty of OR due to the span-uncertainties of O_2 and CO_2 concentrations is expected to be about 1%.

In order to observe the CO_2 flux at the YYG site, the turbulence and the turbulent fluctuation of CO_2 were observed at 52 m with a high time resolution of 10 Hz by using a sonic anemometer (WindMasterPro, Gill) and an open-path infra-red gas analyzer (LI-7500, LI-COR) since November 2012. Turbulent flux of CO_2 was calculated by the eddy correlation method 100 using EddyPro® (Licor) for every 30 minute period. Correlations were applied in the calculation for water-vapor density fluctuation (Webb et al., 1980) and mean vertical wind (Wilczak et al., 2001).

3. Results and discussion

3.1 Variations in the atmospheric O_2 and CO_2 concentrations

We show the 10-minute average values of the atmospheric O_2 and CO_2 concentrations observed at the height of 52 m at 105 YYG in Fig. 2. As seen in the figure, O_2 and CO_2 concentrations vary in opposite phase with each other on timescales ranging from several hours to seasonal cycle. In general, opposite phase variations of atmospheric O_2 and CO_2 are driven by fossil fuel combustion and terrestrial biospheric activities. On the other hand, the atmospheric O_2 variation in $\mu\text{mol mol}^{-1}$ due to the air-sea exchange of O_2 is much larger than that of CO_2 on timescales shorter than 1 year (e.g. Goto et al., 2017a; Hoshina et al., 2018); this is because the equilibration time for O_2 between the atmosphere and the surface ocean is much 110 shorter than that for CO_2 due to the influence of the carbonate dissociation effect on the air-sea exchange of CO_2 (Keeling et al., 1993). Therefore, the opposite phase variations of O_2 and CO_2 observed in this study are attributed mainly to fossil fuel combustion and terrestrial biospheric activities. Figure 2 also shows that ΔO_2 , obtained by subtracting O_2 at 41 m from that at 52 m on the tower, varies in opposite phase with the corresponding ΔCO_2 . High ΔO_2 values are more frequently observed in the winter than in the summer, and short-term (several hours to days) decreases in the O_2 concentration are intense in the 115 winter. Therefore, O_2 is consumed in the urban canopy at YYG, more so in the winter due likely to an increased usage of gas and/or liquid fuels for heating, and to a more stable stratification of surface atmosphere. The daily mean CO_2 flux from the urban area to the overlying atmosphere shown in Fig. 2 shows a seasonal cycle with a wintertime maximum, consistent with the enhancement of O_2 consumption in the urban canopy.

In this study, we focus on the short-term variations of O_2 and CO_2 for periods of several hours to days, to elucidate the O_2 120 and CO_2 exchange processes between the urban area and the atmosphere by examining two types of OR; one is OR_{atm} calculated from a relationship between the O_2 and CO_2 concentration values observed at 52 or 37 m, and the other one is OR_{F} , for the O_2 and CO_2 fluxes between the urban area and the overlying atmosphere, calculated from a relationship between



ΔO_2 and ΔCO_2 . The relationships of the O_2 and CO_2 fluxes with OR_F are based on the aerodynamic method of Yamamoto et al. (1999) by;

125 $F_O = -K \frac{\Delta O_2}{\Delta z}$ (eq.2)

$$F_C = -K \frac{\Delta CO_2}{\Delta z} \quad (\text{eq.3})$$

$$OR_F = -\frac{F_O}{F_C} = -\frac{\Delta O_2}{\Delta CO_2} \quad (\text{eq.4})$$

Here, F_O (F_C) ($\mu\text{mol m}^{-2}\text{s}^{-1}$) represents the O_2 (CO_2) flux from the urban area to the overlaying atmosphere, K is the vertical diffusion coefficient, and $\Delta O_2 \Delta z^{-1}$ ($\Delta CO_2 \Delta z^{-1}$) is the vertical concentration gradient of O_2 (CO_2). The vertical diffusion is a sum of mass-independent eddy and mass-dependent molecular diffusion, however the effect of molecular diffusion on the observed variations of O_2 and CO_2 concentrations is generally negligible in the troposphere, whereas it is significant in the stratosphere (e.g. Ishidoya et al., 2013a). Therefore, we used the same diffusion coefficient K for O_2 and CO_2 in eqs. (2) and (3), which enabled us to estimate F_O by using the observed ΔO_2 , ΔCO_2 and F_C as in eq. (4). In general, OR_{atm} reflects wider footprints of O_2 and CO_2 than OR_F due to horizontal atmospheric transport (Schmid, 1994). It is noted that the definitions of OR_F and OR_{atm} are similar to those of ER_F and ER_{atm} , respectively, reported by Ishidoya et al. (2013b, 2015).

In order to calculate OR_{atm} for short-term variations, (1) we applied a best-fit curve consisting of the fundamental and its first harmonics (periods of 12 and 6 months) and a linear trend to the maxima (minima) values of O_2 (CO_2) observed at 52 m during the successive 1-week periods, and regarded the best-fit curve as its baseline variation, (2) then the baseline variation of O_2 (CO_2) concentration was subtracted from the respective O_2 (CO_2) concentrations observed at 52 m. Figure 3 shows the baseline variations and the variations in the O_2 and CO_2 concentrations observed at Minamitorishima (MNM; 24.28°N, 153.98°E), Japan (updated from Ishidoya et al., 2017). MNM is a small and isolated coral island located 1,850 km southeast of Tokyo, Japan, and the observation site was operated by the Japan Meteorological Agency (JMA) under the Global Atmosphere Watch program of the World Meteorological Organization (WMO/GAW). The baseline variations of O_2 and CO_2 at YYG show clear seasonal cycles with peak-to-peak amplitudes of 28 and 16 $\mu\text{mol mol}^{-1}$, respectively, with corresponding seasonal maximum and minimum appearing in mid August. The amplitude of the seasonal O_2 (CO_2) cycle and the appearance of seasonal maximum (minimum) were found to be larger and earlier, respectively, than those observed at MNM, while the annual average values of the baseline concentration variations of O_2 and CO_2 at YYG did not differ significantly from those at MNM. These characteristics of the seasonal cycles and the annual average values of the baseline variations at YYG and their comparison with those at MNM are generally consistent with those observed at similar latitude over the western Pacific region (Tohjima et al., 2005b). Therefore, in spite of the fact that the YYG site is located in a megacity, the baseline variations of O_2 and CO_2 concentrations are similar to those in the background air.



3.2 O₂:CO₂ exchange ratio and O₂ flux between the urban area and the overlying atmosphere

Figure 4 (a) shows the relationship between all the ΔO_2 and ΔCO_2 values to obtain the average OR_F throughout the observation period in this study. By applying a linear regression analysis to the data, the average OR_F value was calculated to be 1.617 ± 0.004 ($\pm 1\sigma$). The relationship between the O₂ and CO₂ concentration anomalies, calculated by subtracting the respective baseline variations shown in Fig. 3 from the observed O₂ and CO₂ concentrations, is also shown in Fig. 4 (b). By applying a linear regression analysis to the data, we obtained an average OR_{atm} value of 1.540 ± 0.002 ($\pm 1\sigma$) throughout the observation period. Both the OR_F and OR_{atm} values fall within the range of the average OR values of 1.44 for liquid fuels and 1.95 for gas fuels, which suggests that the short-term variations of O₂ and CO₂ concentrations at YYG site were driven mainly by a consumption of liquid and gas fuels rather than terrestrial biospheric activities of which OR is about 1.1 (Severinghaus, 1995). Under a closer inspection, the average OR_F value is slightly but significantly larger than OR_{atm} . As mentioned above, OR_{atm} is an exchange ratio for O₂ and CO₂ concentration anomalies from the baseline variations and reflects sources or sinks of O₂ and CO₂ from a wider footprint area of fossil fuel combustion and terrestrial biospheric activities than the flux footprint for OR_F at YYG. Therefore, the larger average OR_F value than the OR_{atm} value seen in Fig. 4 suggests that a ratio of consumption of gas fuels to liquid fuels, and/or a ratio of fossil fuel combustion to terrestrial biospheric activities, is higher in the urban canopy air at YYG (represented by OR_F) than that in the overlying atmosphere (represented by OR_{atm}).

To examine the seasonal difference between the OR_F and OR_{atm} values, we show the OR_F values calculated by applying regression lines to 1 day and 1 week successive ΔO_2 and ΔCO_2 values in Fig. 5. The corresponding OR_{atm} values, obtained by applying regression lines to successive O₂ and CO₂ concentrations anomalies in Fig. 4 (b), are also shown. Since there is no statistically significant difference between the two (based on the uncertainties shown in the figure ($\pm 1\sigma$)), we focus our discussion on the OR values obtained from the 1 week successive data. Clear seasonal cycles with wintertime maxima are found both in the OR_F and OR_{atm} values at YYG. Larger OR_{atm} values in the winter than in the summer in urban areas have been reported by some past studies (e.g. van der Laan et al., 2014; Ishidoya and Murayama, 2014; Goto et al., 2013), and generally interpreted as a result of the wintertime increase and decrease of fossil fuel combustion and terrestrial biospheric activities, respectively. Biospheric activities included in the summertime and wintertime flux footprints at YYG were 9 and 2%, respectively (Hirano et al., 2015), and there was no significant solid fuel consumption, such as coal-fired power generation plant of which OR is expected to be 1.17 (Keeling, 1988), detected in the footprints. Therefore, the wintertime OR_F was determined mainly by gas and liquid fuels consumption around the YYG site, given that little vegetation and weak terrestrial biospheric activities occurred in the wintertime. If we assume the wintertime OR_F is determined only by gas and liquid fuels consumption, with OR values of 1.95 and 1.44, respectively, then 45% of the CO₂ flux during the December to February (DJF) period was driven by gas fuel consumption, with the rest attributed to liquid fuel consumption. It should be noted that the contributions of gas and liquid fuels are expected to be under- and overestimated since we have ignored the contribution from human respiration with OR values in the range of 1.0 to 1.4. The respiration quotients (the reciprocal of



185 OR) for carbohydrates, lipid and protein are known to be about 1.0, 0.7 and 0.8, respectively. Precise estimation of the contribution of human respiration to the urban OR will be investigated in a future study.

Figure 5 also shows that the OR_F values were systematically larger than OR_{atm} throughout the year, except for October 2016 and July 2017. The average OR_F and OR_{atm} during DJF were 1.67 ± 0.03 and 1.63 ± 0.02 , respectively, both of which agree with the OR value of 1.65 calculated using the statistical data of fossil fuel consumption in Tokyo reported by the Agency of
190 Natural Resources and Energy (<http://www.enecho.meti.go.jp/en/>), assuming OR value of 1.95, 1.44 and 1.17 for gas, liquid and solid fuels consumption, respectively (hereafter referred to as “ OR_{ff} ”). On the other hand, using the same procedure as above, the average OR_{ff} was calculated to be 1.52 ± 0.1 for the Kanto area of about 17,000 km² that includes Tokyo. Therefore, not only OR_F but also OR_{atm} at YYG mainly reflected an influence of the fossil fuel consumption in Tokyo rather than that in the wider Kanto area in the wintertime. On the other hand, both the OR_F and OR_{atm} values in the summer were
195 lower than OR_{ff} in Tokyo (1.65), but OR_{atm} was also found to be lower than OR_{ff} for the Kanto area (1.52). These comparatively lower OR_F and OR_{atm} values than OR_{ff} are attributable to the summertime terrestrial biospheric activities. The lower OR_{atm} than OR_F at YYG throughout the year is probably due to the higher contribution of the air mass from Kanto area to OR_{atm} than OR_F , since the Kanto area as a whole has lower OR_{ff} than for Tokyo; in addition, the south Kanto area (including Tokyo) has a larger vegetation coverage of about 50% than that in the area around YYG site.

200 From the observed OR_F and CO_2 flux, we derived average diurnal cycles of the O_2 flux between the urban area and the overlying atmosphere for each season by using eqs. (2)-(4). Figure 6 shows the average diurnal cycles of ΔO_2 and ΔCO_2 for each season. To derive these seasonal “climatological” diurnal cycles, the observed ΔO_2 and ΔCO_2 values of each day in a season were overlaid on top of the values of other days, added up and divided by the number of days in the season. The error bars shown in Fig. 6 indicate ± 1 standard error (standard deviation from the mean/square route of the data-number).

205 The ΔO_2 and ΔCO_2 values vary systematically in opposite phase and take positive and negative values, indicating transport of O_2 uptake and CO_2 emission signal from the urban area to the overlying atmosphere throughout the year, respectively. Daily maxima of ΔO_2 shown in Fig. 6 are higher in the winter than in the summer and occur in the nighttime. These characteristics would be attributable to an enhancement of the anthropogenic O_2 consumption in the winter, while the nighttime decrease of O_2 concentration would be due to the O_2 consumption near the surface and stable stratification of the
210 surface atmosphere. It must be noted that the ΔCO_2 values in the daytime are nearly zero, while the ΔO_2 values are not. The intercepts of the regression lines fitted to the relationship between ΔO_2 and ΔCO_2 in Fig. 6 are 0.27, 0.41, 0.45 and 0.44 $\mu\text{mol mol}^{-1}$ in DJF, MAM, JJA and SON, respectively. Unfortunately, we did not fix the cause(s) of such biases yet, although it may be related, to some extent, to natural exchange processes between the urban area and the overlying atmosphere. Therefore, because of these issues, the use of OR_F , calculated by applying a regression line to 2-hour period
215 values of ΔO_2 and ΔCO_2 of the climatological diurnal cycle (the number of data included in each 2-hour periods were 400 – 800, depending on the season), to determine the relationship between the O_2 and CO_2 fluxes is preferable. The OR_F values plotted in Fig. 6 show diurnal cycles with daytime minima in DJF, MAM and SON while no clear cycle is found in JJA.



From 10:00 – 16:00 local time, the OR_F values are in the range of 1.44 – 1.59 in all seasons. This suggests that the dominant cause in determining the daytime OR_F is the consumption of gasoline by cars, with OR values of 1.52–1.56 (Keeling, 1988).
220 On the other hand, the OR_F values from 18:00 – 9:00 local time are more variable, in the range of 1.39 – 1.74, and are clearly larger in the winter than in the summer. Therefore, it is suggested that the consumption of gas fuels increases in the winter, especially in the morning and late in the evening, and that the terrestrial biospheric respiration, enhanced in the summer, makes the OR_F values smaller than that expected from liquid fuels consumption alone in JJA. The diurnal OR_F cycles are useful in identifying the causes of CO_2 flux, so that the atmospheric O_2 measurements will provide additional constraint on
225 the CO_2 emission analysis reported in past studies (e.g. Hirano et al., 2015).

The diurnal cycles of the observed CO_2 flux and the estimated O_2 flux from the urban area to the overlying atmosphere are plotted in Fig. 6. The CO_2 flux shows clear diurnal cycles with two peaks for all seasons, one in the morning and the other in the evening. The shape of the diurnal CO_2 flux cycle, with larger flux in the winter than in the summer, was also found in our previous study at YYG for the period 2012–2013 (Hirano et al., 2015). On the other hand, the O_2 flux shows similar diurnal
230 cycles but in opposite phase with the CO_2 flux. The daily mean CO_2 fluxes were 15.6 ± 0.2 , 11.2 ± 0.1 , 9.3 ± 0.1 and $11.5 \pm 0.1 \mu\text{mol m}^{-2}\text{s}^{-1}$ in DJF, MAM, JJA and SON, respectively, while the respective daily mean O_2 fluxes were -25.4 ± 0.3 , -17.8 ± 0.2 , -14.1 ± 0.2 and $-17.7 \pm 0.2 \mu\text{mol m}^{-2}\text{s}^{-1}$. Steinbach et al. (2011) reported a global dataset of CO_2 emissions and O_2 uptake associated with fossil fuel combustion using the EDGAR inventory with country level information on OR , based on the fossil fuel consumption data from the UN energy statistics database. The O_2 uptake around Tokyo for the year 2006 was
235 seen from Fig. 2 in Steinbach et al. (2011) to be about $e^{16} - e^{17} \text{ kgO}_2 \text{ km}^{-2}\text{year}^{-1}$, which corresponds to $-9 - -24 \mu\text{mol m}^{-2}\text{s}^{-1}$ of O_2 flux and is consistent with those observed in this study.

It is well known that the atmospheric O_2 concentration has been observed to show a secular decrease (e.g. Keeling and Manning, 2014), and the change rate was about $-4 \mu\text{mol yr}^{-1}$ for the period 1996 – 2013, while the secular change rate of CO_2 concentration for the period was about $2 \mu\text{mol yr}^{-1}$ (Goto et al., 2017b). The O_2 change rate of $-4 \mu\text{mol yr}^{-1}$ corresponds to -
240 $0.04 \mu\text{mol m}^{-2}\text{s}^{-1}$ of O_2 (CO_2) flux, assuming $5.1 \times 10^{14} \text{ m}^2$ for the surface area of the earth, $5.124 \times 10^{21} \text{ g}$ for the total mass of dry air (Trenberth, 1981) and 28.97 g mol^{-1} for the mean molecular weight of dry air. Therefore, the annual mean O_2 consumption rate of $-16.3 \mu\text{mol m}^{-2}\text{s}^{-1}$ at YYG reported in this study is more than 350 times larger than the global mean consumption rate. If the total land surface consumes O_2 with a comparable rate found at YYG and the ocean is assumed to be O_2 neutral, then it would take only 70 years to reduce the atmospheric O_2 concentration to 18%, causing global deficiency in
245 oxygen for human beings. Although this is an unrealistic speculation, it does show the extent of anthropogenic consumption of atmospheric O_2 , and forces us to recognize the fact that our city life is not sustainable, not only in terms of CO_2 emission associated with global warming but also from a viewpoint of the conservation of atmospheric O_2 to survive.



4. Conclusions

Continuous simultaneous observations of atmospheric O₂ and CO₂ and CO₂ flux have been carried out at the YYG site, Toyo,
250 Japan since March 2016. Sample air was taken from air intakes set at heights of 52 m and 37 m of the YYG tower, allowing
us to apply an aerodynamic method by using the vertical gradients of the O₂ and CO₂ concentration measurements. We
compared OR_F obtained from the aerodynamic method with OR_{atm}, representing OR of the overlying atmosphere above the
urban canopy. We found clear seasonal variations with wintertime maxima for both OR_F and OR_{atm}, as well as slightly
higher OR_F than OR_{atm} throughout the year. The annual mean OR_F and OR_{atm} were observed to be 1.62 and 1.54,
255 respectively, falling within the range of the respective average OR values of 1.44 and 1.95 of liquid and gas fuels. Larger
OR_{atm} values in the winter than the summer were interpreted generally as reflecting the wintertime increase and decrease in
fossil fuel combustion and terrestrial biospheric activities, respectively. The slightly lower OR_{atm} than OR_F in the summer
was probably due to an influence of the air mass from the wider Kanto area to OR_{atm} at YYG since the OR value of 1.1 for
the terrestrial biospheric activities is lower than those for liquid and gas fuels consumption; in addition, the influence of the
260 vegetation included in the flux footprints at YYG was much smaller than that in the surrounding Kanto area.

Seasonal variations were seen in the average diurnal OR_F cycles, showing daytime minima in DJF, MAM and SON, while
no clear diurnal cycle was distinguishable in JJA. The OR_F values were more variable seasonally in the nighttime than
daytime, and the nighttime OR_F was clearly larger in the winter than in the summer, probably due not only to an increase in
the consumption of gas fuels in winter, especially in the morning and late in the evening, but also to the enhanced terrestrial
265 biospheric respiration in the summer. The daily mean O₂ flux values at YYG were about -25 and -14 μmol m⁻²s⁻¹ in the
winter and the summer, respectively. The annual mean O₂ flux of -16.3 μmol m⁻²s⁻¹ was more than 350 times larger than the
global mean consumption rate of atmospheric O₂ reported by past studies. This highlights the impact of global urbanization
and the unsustainability of the dependency on fossil fuel.

270 *Data availability.*

The data at YYG site presented in this study can be accessed by contacting the corresponding author.

Author contributions.

SI designed the study and drafted the manuscript. Measurements of O₂ concentrations, CO₂ concentrations, and CO₂ flux
275 were conducted by SI, SI and YT, and HS, respectively. NA prepared standard gas for the O₂ measurements. SI and KT
conducted O₂ observations at MNM. HS, NK and HK examined the results and provided feedback on the manuscript. All the
authors approved the final manuscript.

Competing interests.

280 The authors declare that they have no conflict of interest.



Acknowledgements.

We thank Prof. T. Nakajima at Tokai University, Dr. Shohei Murayama and JANS Co. Ltd. for supporting the observation. This study was partly supported by the JSPS KAKENHI Grant Number 24241008, 15H02814 and 18K01129, and the
285 Environment Research and
Technology Development Fund (1-1909) and the Global Environment Research Coordination System from the Ministry of the Environment, Japan.

References

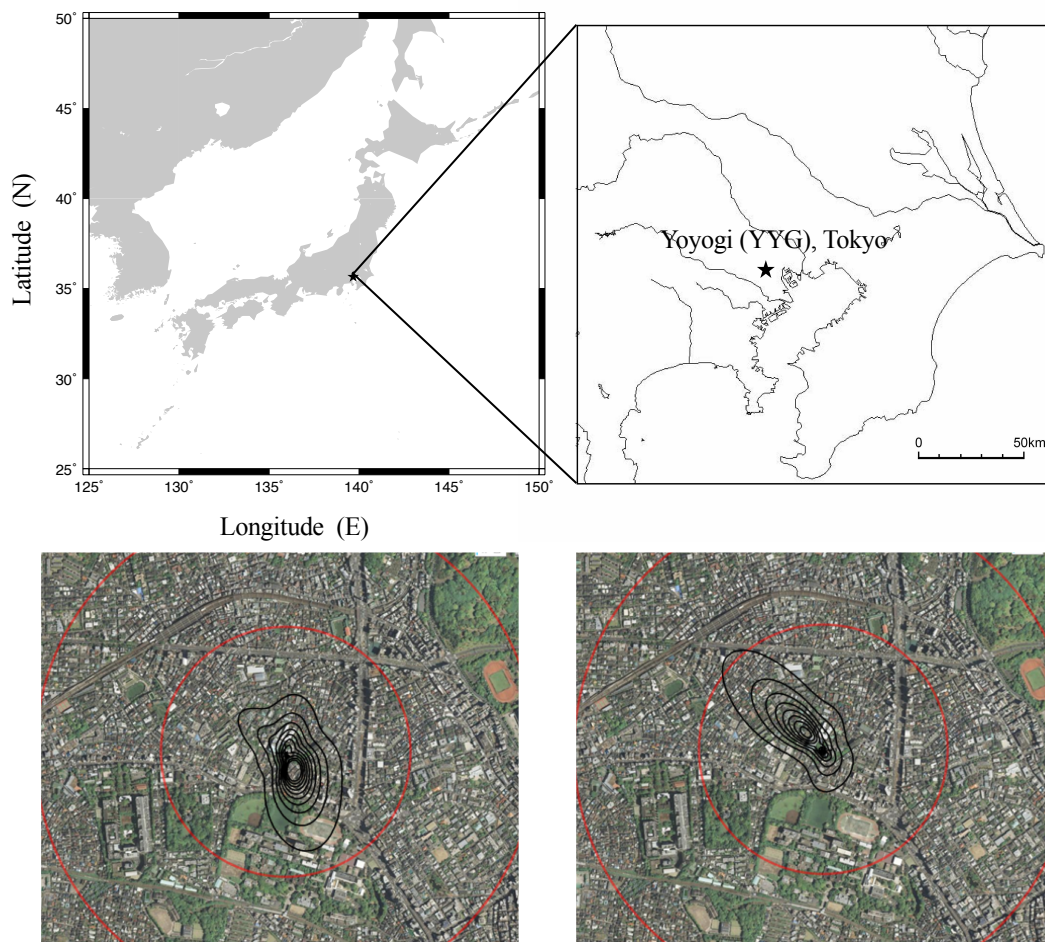
- Aoki, N., Ishidoya, S., Mastumoto, N., Watanabe, T., Shimosaka, T., and Murayama, S.: Preparation of primary standard
290 mixtures for atmospheric oxygen measurements with uncertainty less than 1 ppm for oxygen mole fractions, *Atmos. Meas. Tech.*, 12, 2631–2646, 2019.
- Goto, D., Morimoto, S., Ishidoya, S., Ogi, A., Aoki, S., and Nakazawa, T.: Development of a high precision continuous measurement system for the atmospheric O₂/N₂ ratio and its application at Aobayama, Sendai, Japan, *J. Meteorol. Soc. Japan*, 91, 179-192, 2013.
- 295 Goto, D., Morimoto, S., Aoki, S., Patra, P. K., and Nakazawa, T.: Seasonal and short-term variations in atmospheric potential oxygen at Ny-Ålesund, Svalbard, *Tellus 69B*, 1311767, DOI: 10.1080/16000889.2017.1311767, 2017a.
- Goto, D., Morimoto, S., Ishidoya, S., Aoki, S., and Nakazawa, T.: Terrestrial biospheric and oceanic CO₂ uptake estimated from long-term measurements of atmospheric CO₂ mole fraction, δ¹³C and δ(O₂/N₂) at Ny-Ålesund, Svalbard, *J. Geophys. Res. Biogeosci.*, 122, doi:10.1002/2017JG003845, 2017b.
- 300 Hirano, T., Sugawara, H., Murayama, S., and Kondo, H.: Diurnal variation of CO₂ flux in an urban area of Tokyo, *SOLA*, 11, 100–103, 2015.
- Hoshina, Y., Tohjima, Y., Katsumata, K., Machida, T., and Nakaoka, S.: In situ observation of atmospheric oxygen and carbon dioxide in the North Pacific using a cargo ship, *Atmos. Chem. Phys.*, 18, 9283-9295, 2018.
- Ishidoya, S., Sugawara, S., Morimoto, S., Aoki, S., Nakazawa, T., Honda, H., and Murayama, S.: Gravitational separation in
305 the stratosphere – a new indicator of atmospheric circulation, *Atmos. Chem. Phys.*, 13, 8787–8796, 2013a.
- Ishidoya, S., Murayama, S., Takamura, C., Kondo, H., Saigusa, N., Goto, D., Morimoto, S., Aoki, N., Aoki, S., and Nakazawa, T.: O₂:CO₂ exchange ratios observed in a cool temperate deciduous forest ecosystem of central Japan, *Tellus B*, 65, 21120, <http://dx.doi.org/10.3402/tellusb.v65i0.21120>, 2013b.
- Ishidoya, S., and Murayama, S.: Development of high precision continuous measuring system of the atmospheric O₂/N₂ and
310 Ar/N₂ ratios and its application to the observation in Tsukuba, Japan, *Tellus 66B*, 22574, <http://dx.doi.org/10.3402/tellusb.v66.22574>, 2014.



- Ishidoya, S., Murayama, S., Kondo, H., Saigusa, N., Kishimoto-Mo, A. W., Yamamoto, S.: Observation of O₂:CO₂ exchange ratio for net turbulent fluxes and its application to forest carbon cycles, *Ecol Res*, 30, 225–234, 2015.
- Ishidoya, S., Tsuboi, K., Murayama, S., Matsueda, H., Aoki, N., Shimosaka, T., Kondo, H., and Saito, K.: Development of a
315 continuous measurement system for atmospheric O₂/N₂ ratio using a paramagnetic analyzer and its application in Minamitorishima Island, Japan, *SOLA*, 13, 230-234, 2017
- Keeling, C. D., Piper, S. C., Whorf, T. P., and Keeling, R. F.: Evolution of natural and anthropogenic fluxes of atmospheric CO₂ from 1957 to 2003, *Tellus*, 63B, 1-22, 2011.
- Keeling, R. F.: Development of an Interferometric Oxygen Analyzer for Precise Measurement of the Atmospheric O₂ Mole
320 Fraction, PhD Thesis. Harvard University, Cambridge, 1988.
- Keeling, R. F., and Shertz, S. R.: Seasonal and interannual variations in atmospheric oxygen and implications for the global carbon cycle, *Nature*, 358, 723-727, 1992.
- Keeling, R. F., Bender, M. L., and Tans, P. P.: What atmospheric oxygen measurements can tell us about the global carbon cycle, *Global Biogeochem. Cycles*, 7, 37-67, 1993.
- 325 Kljun, N., Calanca, P., Rotach, M. W., Schmid, H. P.: A simple parameterisation for flux footprint predictions, *Bound.-Layer Meteorol.*, 112, 503-523, 2004.
- Machida, T., Tohjima, Y., Katsumata, K., and Mukai, H.: A new CO₂ calibration scale based on gravimetric one-step dilution cylinders in National Institute for Environmental Studies-NIES 09 CO₂ scale, Paper presented at: Report of the 15th WMO Meeting of Experts on Carbon Dioxide Concentration and Related Tracer Measurement Techniques;
330 September 2009; Jena, Germany, (WMO/GAW Rep. 194, edited by: Brand, W., 165-169, WMO, Geneva, Switzerland), 2011.
- Miller, J. B., and Tans, P. P.: Calculating isotopic fractionation from atmospheric measurements at various scales, *Tellus B*, 55, 207-214, 2003.
- Mitchell, L. E., Lin, J. C., Bowling, D. R., Pataki, D. E., Strong, C., Schauer, A. J., Bares, R., Bush, S. E., Stephens, B. B.,
335 Mendoza, D., Mallia, D., Holland, L., Gurney, K. R., Ehleringer, J. R.: Long-term urban carbon dioxide observations reveal spatial and temporal dynamics related to urban characteristics and growth, *Proceedings of the National Academy of Sciences*, 115, 2912-2917, doi: 10.1073/pnas.1702393115, 2018.
- Nakazawa, T., Aoki, S., Murayama, S., Fukabori, M., Yamanouchi, T., and Murayama, H.: The concentration of atmospheric carbon dioxide at Japanese Antarctic station, Syowa, *Tellus*, 43B, 126-135, 1991.
- 340 Schmid, H. P.: Source areas for scalars and scalar fluxes, *Bound.-Layer Meteorol.*, 67, 293–318, 1994.
- Severinghaus, J.: Studies of the terrestrial O₂ and carbon cycles in sand dune gases and in biosphere 2, Ph. D. thesis, Columbia University, New York, 1995.
- Song, T., and Wang, Y.: Carbon dioxide fluxes from an urban area in Beijing, *Atmospheric Research*, 106, 139–149, 2012.



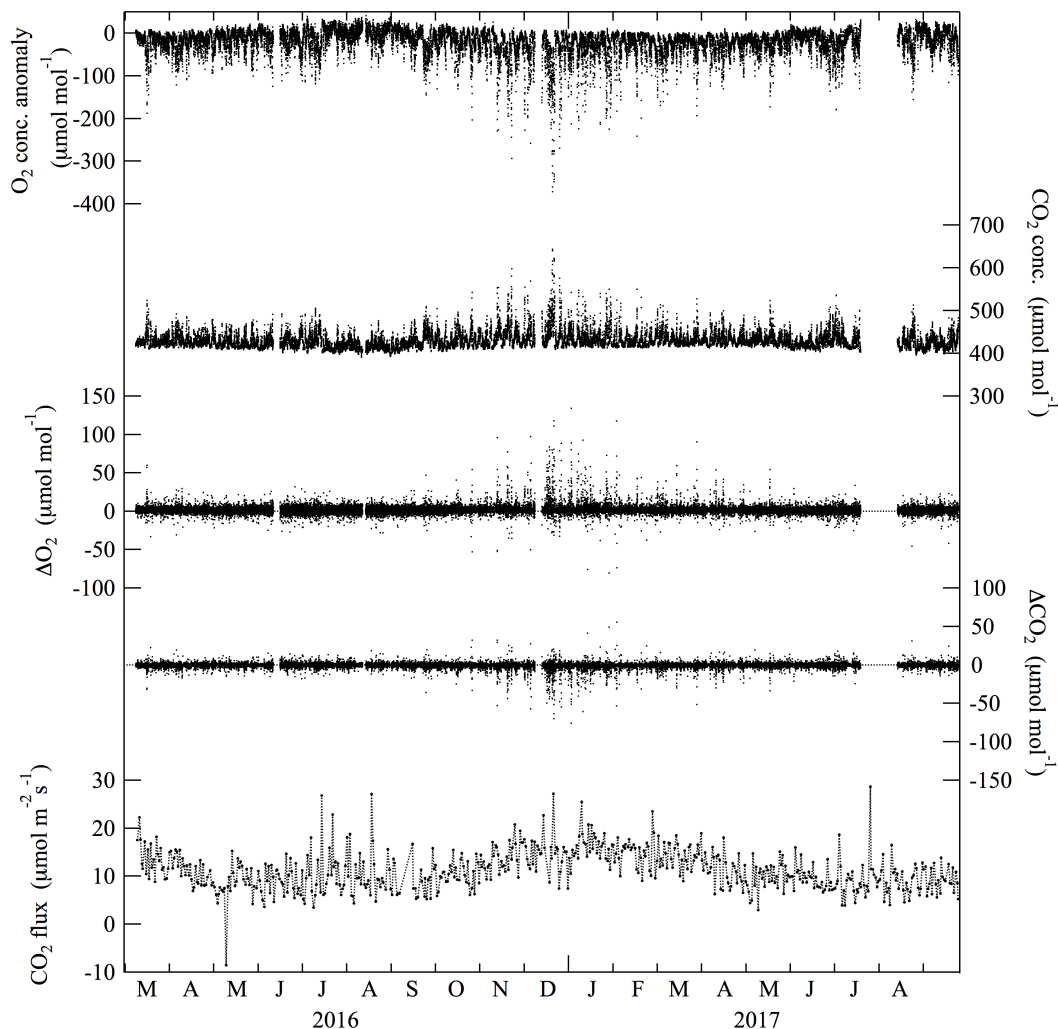
- Steinbach, J., Gerbig, C., Rödenbeck, C., Karstens, U., Minejima, C., and Mukai, H.: The CO₂ release and oxygen uptake
345 from fossil fuel emission estimate (COFFEE) dataset: effects from varying oxidative ratios, *Atmos. Chem. Phys.*, 11,
6855-6870, 2011.
- Tohjima, Y., Machida, T., Watai, T., Akama, I., Amari, T., and Moriwaki, Y.: Preparation of gravimetric standards for
measurements of atmospheric oxygen and re-evaluation of atmospheric oxygen concentration, *J. Geophys. Res.*, 110,
D11302, doi:10.1029/2004JD005595, 2005a.
- 350 Tohjima, Y., Mukai, H., Machida, T., Nojiri, Y., and Gloor, M.: First measurements of the latitudinal atmospheric O₂ and
CO₂ distributions across the western Pacific, *Geophys. Res. Lett.*, 32, L17805, doi:10.1029/2005GL023311, 2005b.
- Trenberth, K. E.: Seasonal variations in global sea level pressure and the total mass of the atmosphere. *J. Geophys. Res.*,
86(C6), 5238-5246, 1981.
- Velasco, E., Pressley, S., Grivicke, R., Allwine, E., Coons, T., Foster, W., Jobson, B. T., Westberg, H., Ramos, R.,
355 Hernández, F., Molina, L. T., and Lamb, B.: Eddy covariance flux measure- ments of pollutant gases in urban Mexico
City, *Atmos. Chem. Phys.*, 9, 7991-8034, 2009.
- van der Laan, S., van der Laan-Luijkx, I. T., Zimmermann, L., Conen, F., and Leuenberger, M.: Net CO₂ surface emissions
at Bern, Switzerland inferred from ambient observations of CO₂, $\delta(\text{O}_2/\text{N}_2)$, and ²²²Rn using a customized radon tracer
inversion, *J. Geophys. Res. Atmos.*, 119, 1580-1591, doi:10.1002/ 2013JD020307, 2014.
- 360 Ward, H. C., Evans, J. G., and Grimmond, C. S. B.: Multi-season eddy covariance observations of energy, water and carbon
fluxes over a suburban area in Swindon, UK, *Atmos. Chem. Phys.*, 13, 4645-4666, 2013.
- Webb, E. K., Pearman, G. I., and Leuning, R.: Correction of flux measurements for density effects due to heat and water
vapor transfer, *Q. J. R. Meteorol. Soc.*, 106, 85-100, 1980.
- Wilczak, J. M., Oncley, S. P., and Stage, S. A.: Sonic anemometer tilt correction algorithms, *Bound.-Layer Meteorol.*, 99,
365 127-150, 2001.
- Yamamoto S., Murayama, S., Saigusa, N., and Kondo, H.: Seasonal and inter-annual variation of CO₂ flux between a
temperate forest and the atmosphere in Japan. *Tellus*, 51B, 402-413, 1999.



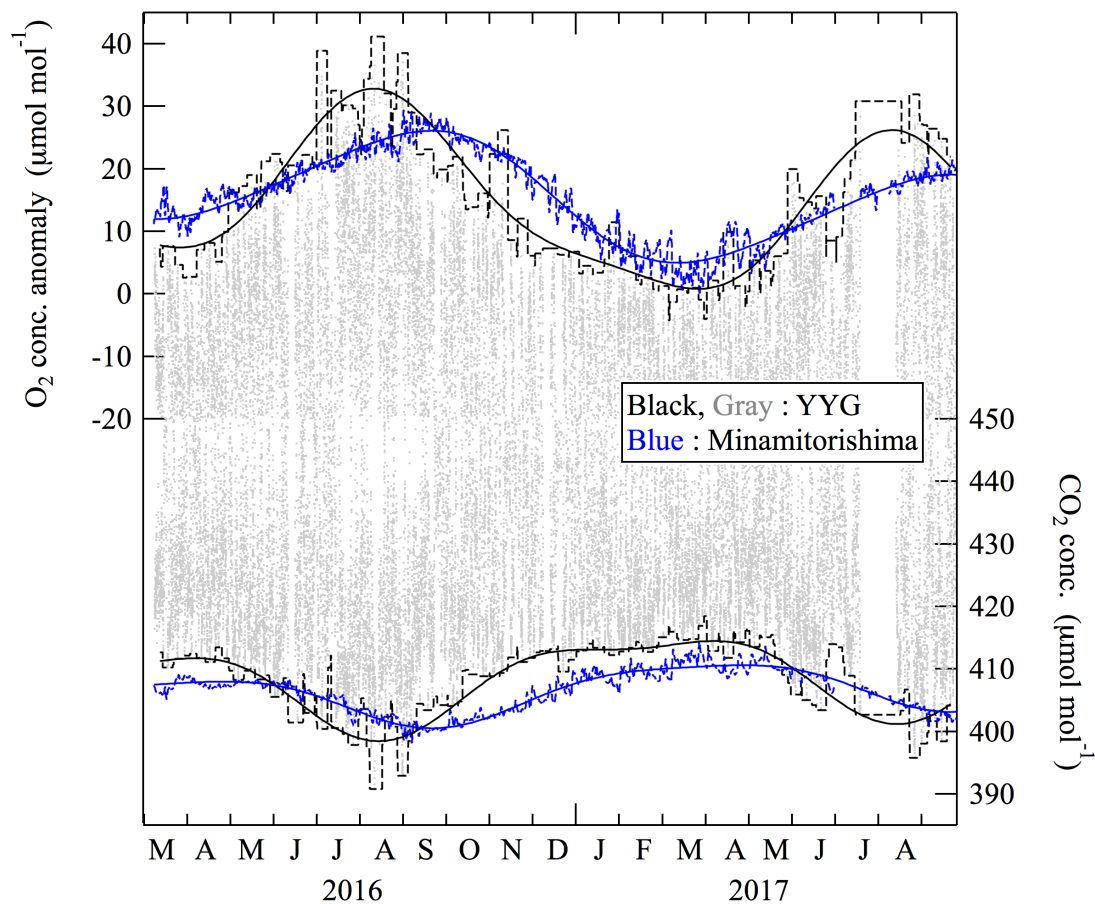
370

Figure 1: Upper panel: Location of the Yoyogi site (35.66°N , 139.68°E , YYG), Tokyo, Japan. Lower panel: Aerial photo from the Geospatial Information Authority of Japan around the study area at YYG. Typical flux footprints in the summer (left) and the winter (right) are also shown by black circles. Inside and outside the red circles indicate the distance of 500 m and 1000 m, respectively, from a roof-top tower of Tokai University where the observations of O_2 and CO_2 concentrations and CO_2 flux were carried out.

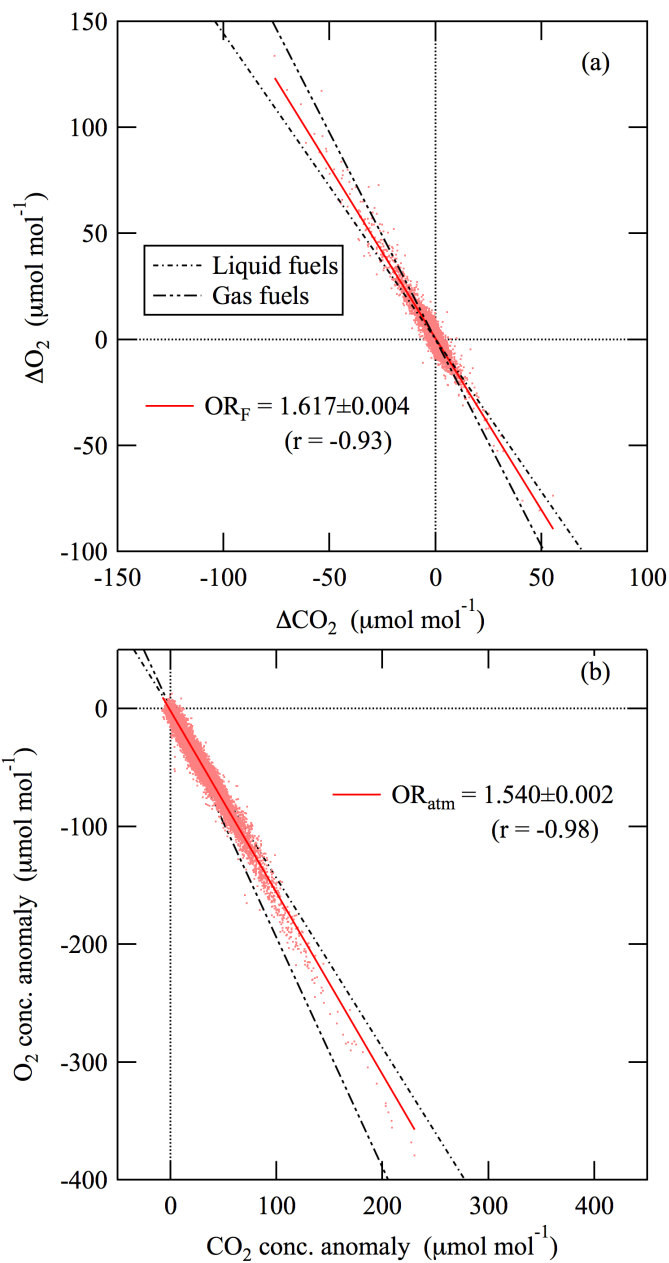
375



380 **Figure 2:** Variations in O_2 and CO_2 concentrations observed at the tower height of 52 m at Yoyogi, Tokyo, Japan for the period March 2016 – September 2017. The O_2 concentrations are expressed as deviations from the value observed at 9:58 on March 9, 2016. ΔO_2 , representing the differences calculated by subtracting the observed O_2 concentrations at 37 m from that at 52 m, are also shown. ΔCO_2 are the same as ΔO_2 but for CO_2 concentration. Daily mean CO_2 fluxes observed using the eddy correlation method are also shown, and the flux takes on positive value when the urban area emits CO_2 to the overlying atmosphere.



385 Figure 3: Baseline variations of O₂ and CO₂ concentrations at the tower height of 52 m at Yoyogi, Tokyo, Japan, represented by their best-fit curves (black solid lines) to the respective maxima and minima values during the successive 1-week periods (black dashed lines). Variations of 24 hours-averaged O₂ and CO₂ concentrations at Minamitorishima, Japan (blue dashed line) and their best-fit curves (blue solid lines) are also shown (updated from Ishidoya et al., 2017).



390

Figure 4: (a) Relationship between the ΔO_2 and ΔCO_2 shown in Fig. 2. Average OR_F (see text) for the observation period, derived from the regression line fitted to the data is also shown. (b) Same as in (a) but for the deviations of O₂ and CO₂ concentrations from their baseline variations shown in Fig. 3 and the average OR_{atm} (see text). OR values expected from the consumptions of gas and liquid fuels are also shown.

395

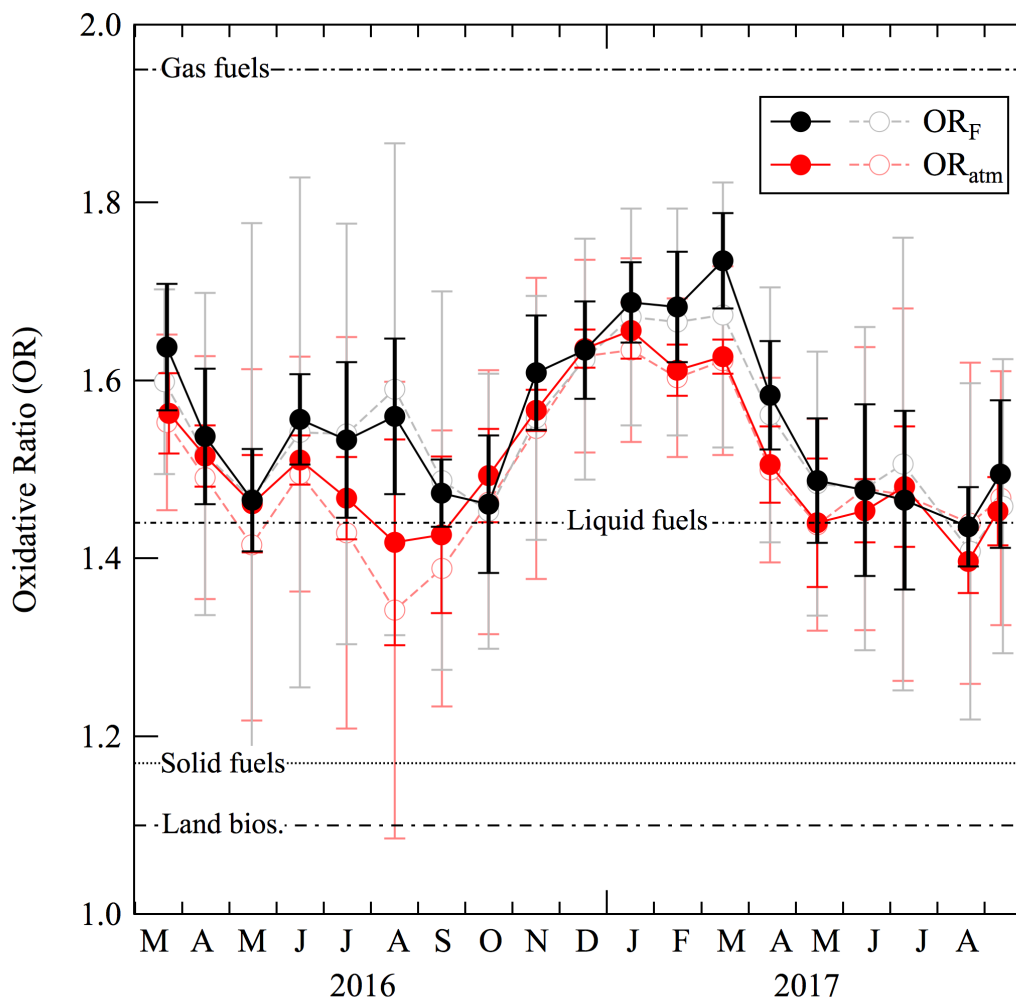
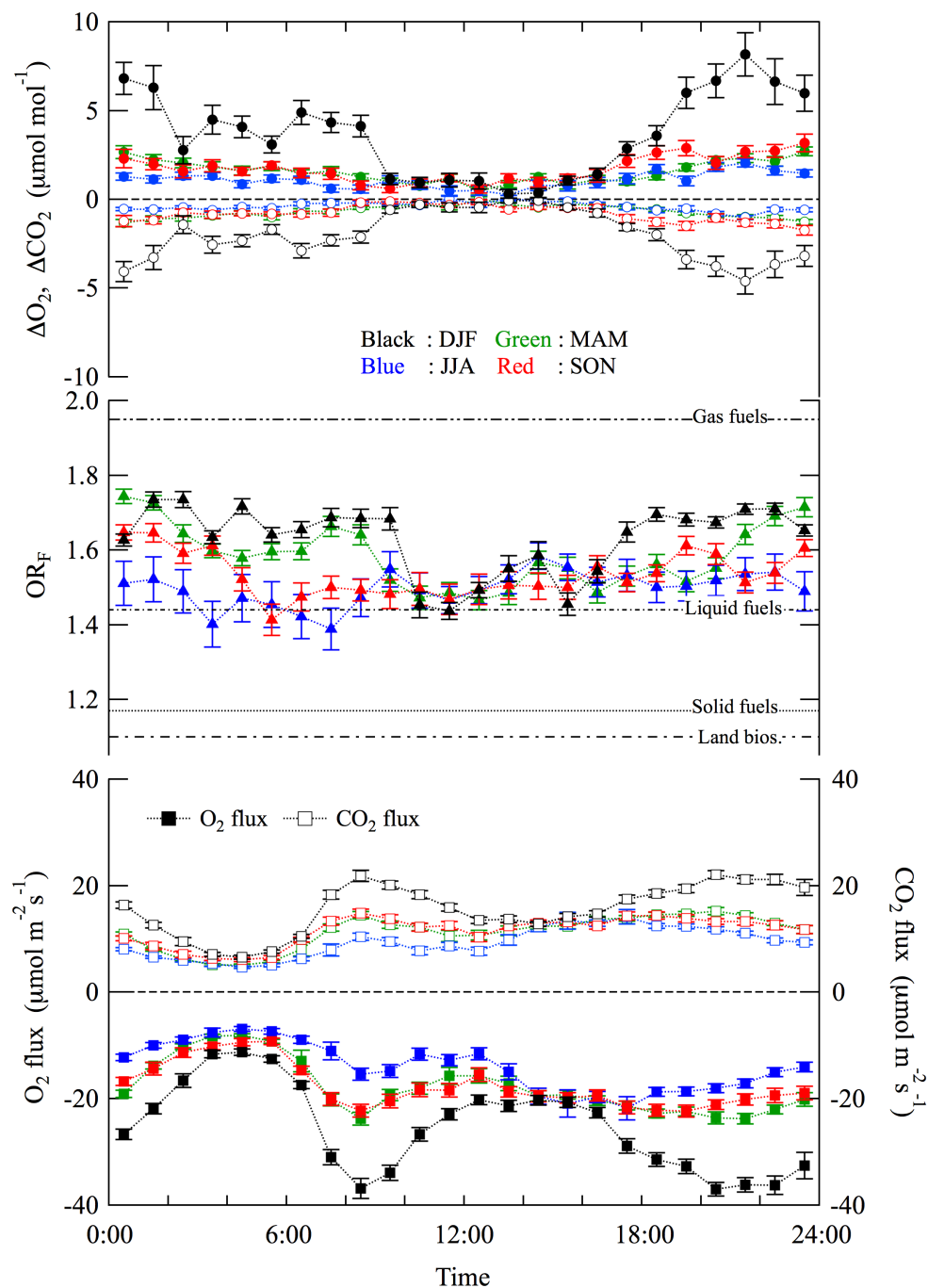


Figure 5: OR_F calculated by applying regression lines to 1 day (gray open circles) and 1 week (black closed circles) successive ΔO_2 and ΔCO_2 values. Also plotted are OR_{atm} calculated by applying regression lines to 1-day (light red open circles) and 1-week (dark red closed circles) successive O_2 and CO_2 deviations from their baseline variations shown in Fig. 3. OR values expected from the consumptions of gas, liquid and solid fuels and land biospheric activities are also shown.

400



405 **Figure 6:** Plots of average diurnal cycles of ΔO_2 and ΔCO_2 for each season: December to February (black), March to May (green), June to August (blue) and September to November (red). Average diurnal cycles of OR_F , calculated by applying regression lines to the 2-hour period values of ΔO_2 and ΔCO_2 , are also plotted seasonally (see text). Average diurnal cycles of the CO_2 flux observed using the eddy correlation method, and those of the O_2 flux calculated from the CO_2 flux and OR_F values are also plotted seasonally. Error bars indicate ± 1 standard error.